metals

MDPI

Article

Mechanical and Corrosion Behavior of Al-Zn-Cr Family Alloys

Ahmed Nassef [1], Waleed H. El-Garaihy [2,3,*] and Medhat El-Hadek [1]

[1] Department of Production Engineering & Mechanical Design, Faculty of Engineering, Port-Said University, Port Fouad 42523, Egypt; nassef12@eng.psu.edu.eg (A.N.); melhadek@eng.psu.edu.eg (M.E.-H.)
[2] Mechanical Engineering Department, Unaizah College of Engineering, Qassim University, Unaizah 51911, Saudi Arabia
[3] Mechanical Engineering Department, Faculty of Engineering, Suez Canal University, Ismailia 41522, Egypt
* Correspondence: W.Nasr@qu.edu.sa; Tel.: +966-55-110-8490

Academic Editor: Manoj Gupta
Received: 9 February 2017; Accepted: 3 May 2017; Published: 12 May 2017

Abstract: Aluminum base alloys containing chromium (Cr) and zinc (Zn) were produced using extrusion and powder metallurgy techniques. Cr additions ranged between 5 to 10 wt. %, while Zn was added in an amount between 0 and 20 wt. %. Heat treatment processes were performed during powder metallurgy process, at different temperatures, followed by water quenching. Similar alloys were extruded with an extrusion ratio of 4.6 to get proper densification. Optical microscopy was used for microstructure investigations of the alloys investigated. The element distribution microstructure study was carried out using the Energy Dispersive X-ray analysis method. Hardness and tensile properties of the investigated alloys have been examined. Wear resistance tests were carried out and the results were compared with these of the Al-based bulk alloys. Results showed that the aluminum base alloys, containing 10 wt. % Cr and heat treated at 500 °C for one hour followed by water quenching, exhibited the highest wear resistance and better mechanical properties.

Keywords: Al-Zn-Cr alloys; powder metallurgy; strengthening; extrusion; dry sliding wear

1. Introduction

Aluminum chrome matrix composites (ACMC) are used in a wide range of industries including transportation, electronics, leisure, and others [1–4]. ACMC are usually produced by mechanical alloying of different kinds of metal powders using compression, at a temperature near room temperature, which results in nanocrystalline and supersaturated alloy powders at low temperatures [3]. The large mechanical energies introduced into the powder particles are nanocrystalline interfaces, amorphous state, and promoted reactions between the metals in solid state [5–7]. Studies on the trinity Al-Zn-Cr alloys are very limited throughout the literature. Recently, Kurtuldu et al. have investigated the effect of trace addition on the aging behavior of aluminum alloys containing Cr; moreover, the effect of Cr addition on Zn diffusions in molten of Al-Zn-Cr alloys [8,9]. It has been a subject of interest that minor and trace additives have a noticeable effect on these alloys, as far as structure and tensile properties are concerned [10]. In view of the outstanding corrosion and oxidation resistance, the strengthening and toughening of these alloys have been of recent concern [7–11]. Running experiments on the Al-Cr-Zn system at 600 °C, eleven three-phase regions had been identified [12]. Li et al. studied the effect of grain structure on quench sensitivity of an Al-Zn-Mg-Cu-Cr alloy. The results showed that the decrease of the quenching rate from 960 °C/s to 2 °C/s revealed a decrease in the hardness after aging, for the homogenized and solution heat treated alloy with large equiaxed grains. For the extruded and solution heat treated alloy, elongated grains and subgrains had dominated [13]. The Al-based alloys, with additives of magnesium (Mg) and silicon

(Si), belong to wrought aluminum alloys which are heat treated. It is worth mentioning that there is an increase in the mechanical strength of the alloys with the increase of Mg and Si contents to the solubility limits; on the other hand, the ductility is reduced. Small amounts of Mg, Cr, Zn, Zr or Ti were added to modify the microstructure to improve the mechanical properties, formability, and corrosion resistance of the alloy [14–17]. Enhanced wear and corrosion resistance is considered to be one of the most important attributes of AMC that contain ceramic particles for engineering applications [18]. A progressive degradation of material occurs when two sliding surfaces come in contact; this process is known as wear. Such interaction between surfaces gives rise to friction. Wang et al. [19] studied the effect of additives, such as copper (Cu) and silicon carbide (SiC), on Al-based alloys. Aluminum alloy matrices, with particulates of Al_2O_3 or SiC reinforcements, possess higher strength and stiffness as well as, greater wear resistance and improved high properties [20,21]. On the other hand, the effects of other reinforcement particles such as Cr, Fe, and so on have been studied.

In the present work, the control and optimization of the production processing parameters were implemented through suitable die design compaction with dense powder metallurgy (PM) parts. Using a cold pressed powder metallurgical process, the alloys were manufactured with controlled alloy constitutions using two techniques. The first is based on adopting cold compaction followed by heat treatment at 500 °C. In the second technique, and in order to reduce the grain coarsening resulting from the heat treatment process, similar cold compacted and heat treated alloys were subjected to an extrusion process followed by solution heat treatment and quenching in room temperature water. The influence of adding Zn and various percentages of Cr to aluminum alloys on the density, tensile behavior, hardness, corrosion, and wear resistance of the Al-based alloys was examined; in addition, the effect of production methods on those properties was also inspected.

2. Materials and Methods

Materials with desirable characteristics were attained due to the strong ionic interatomic bonding of Cr and Zn. Powders with purity greater than 99%, with an average particle size less than 50 μm in diameter and manufactured by CNPC powder (Charlottetown, PE, Canada), were used as the starting source materials. The aluminum metallic powder was obtained from ALDRICH (Darmstadt, Germany). Al-based alloys with different compositions were prepared using a mechanical mixer to achieve the needed composition. Six different compositions were prepared namely, Al-5Cr, Al-7.5Cr, Al-10Cr, Al-20Zn, Al-20Zn-5Cr, and Al-20Zn-10Cr. Two techniques were implemented to perform this work. The first uses cold compaction then heat treatment, and the second adopt extrusion followed by solution heat treatment to reduce the grain coarsening resulted from heat treatment process. In the first technique, each powder mixture was cold pressed using a compaction pressure of 425 MPa on the 30 mm diameter billets. The material properties are expected to be diverse since the melting temperatures of Al is around 660 °C, Cr 1900 °C and Zn 420 °C. The powder density of Al is 7190 kg/m^3, Cr is 2700 kg/m^3, and Zn is 7140 kg/m^3. A hydraulic testing machine of 40 Tons capacity was used to perform the compaction of the alloy powder, with constant cross head velocity of 0.002 m/min. The height of green compact was directly measured before and after die ejection. The final height is calculated from the load-displacement curve. After unloading, the elastic recovery of the compacts is neglected [4]. A compacting pressure ranging from 227 to 909 MPa was calculated, by assuming that the cross-section of the compact is equal to that of the die. The temperature of the die was measured using NiCr-Ni thermocouple, which is inserted into the die and maintained at the die cavity. After cold pressing, all of the MMCs alloys were heat–treated at about 500 °C to allow the atoms to diffuse randomly into a uniform solid solution, as liquid phase sintering [4,7]. The tin melts to form a thin film surrounding the copper particles enhancing the alloying element bonding [7]. All alloys were then heat treated to 500 °C for duration of 60 min.

On the other hand, the second technique uses the same alloy powders with different manufacturing steps. It starts with an extrusion process for alloy powders, with an extrusion ratio of 4.6 to get proper densification. The behavior of the extruded alloy was consequently studied.

The extruded bars were subjected to solution treatment temperature of 500 °C for 60 min and then quenched in room temperature water. As the size of the small particle with high curvature increases, the differences in free energy across the curved surface increases, as discussed in [22,23]. The setup was heated to the predefined temperature level and maintained constant for 30 min, to guarantee homogenous distribution within the powder alloy. The forming pressure was then lowered for all tested hot components. After the compact operation, the samples were covered with aluminum foil and embedded in a graphite powder to protect their surface from oxygen and nitrogen from atmosphere, during the sintering process. The specimens were sintered at a steady heating rate of 20 °C/min up to 500 °C for one hour. The temperature was maintained at that level with a tolerance of ±5 °C.

3. Results and Discussion

3.1. Densification Behavior

The relative density densification behaviors of the investigated Al-based alloys as affected by sintering temperature for different percentage of Cr and Zn are shown in Figure 1. From Figure 1 it is clear that the relative density increases by increasing the sintering temperature for the aluminum alloy reinforced with different percentages of Cr and Zn. Three classes of mechanisms contribute to densification: plastic yielding, low power creep, and various sorts of diffusion. In the absence of an external pressure, only the diffusion mechanisms exist as sintering is applied. Pore dragging and pore separation from the pores tend to inhabit the diffusion contribution. In order to take the initial pressed density into consideration, the compact sinterability was computed in terms of densification parameter (ΔD) as a proportional function of (sintered − green)/(theoretical − green) densities. The theoretical density was estimated using theory of mixtures [4,7]. Theoretical solid densities, normalized by after extrusion density of all produced parts, are shown in Figure 2. Higher relative densities (RD) were achieved for hot extruding samples to around 99% from the solid density values. Zn particles, having a distinctive lubricating effect, will enhance to a great extent the packing loss of the powders and retard the sealing for the individual pores. Consequently, density will decrease with Zn addition. This may be liquid Zn diffused inside the aluminum matrix and leaves pore inside the matrix. For the Al-based alloys, Cr particles were observed in the microstructure after heat treatment at 500 °C for one hour followed by water quenching. No difference in the microstructures was observed for these alloys that are heated treated at 500 °C for one hour followed by water quenching, as shown in Figure 3. From the microstructures of the heat treated samples, Al-5Cr homogeneous structure was observed at a temperature of 500 °C followed by water quenching. It should be noted that, with the decrease of the aluminum content in the Al-based alloys and the increase of the Cr and Zn content, the density increases accordingly.

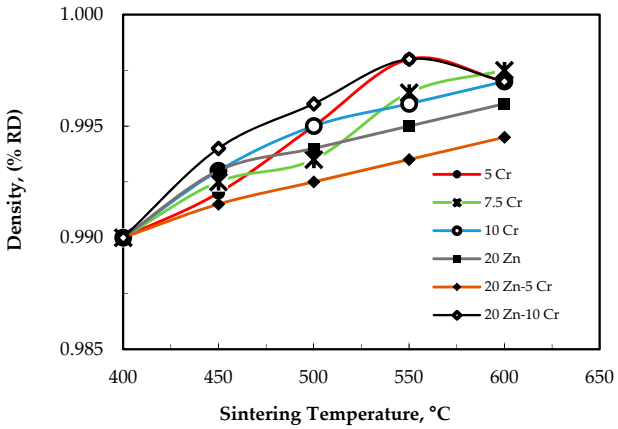

Figure 1. The effect of the sintering temperature on the relative density for different Al-base alloys.

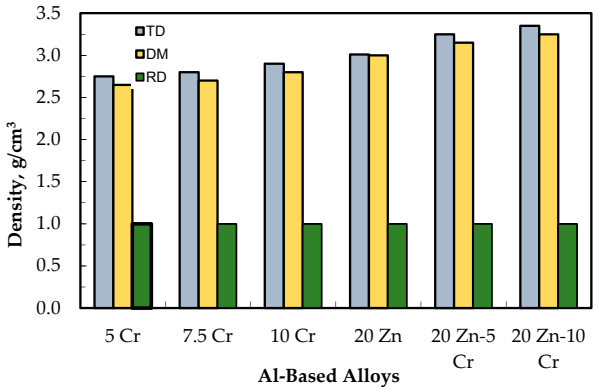

Figure 2. The density of as extruded Al-base alloys (TD theoretical density, DM density measured, and RD relative density).

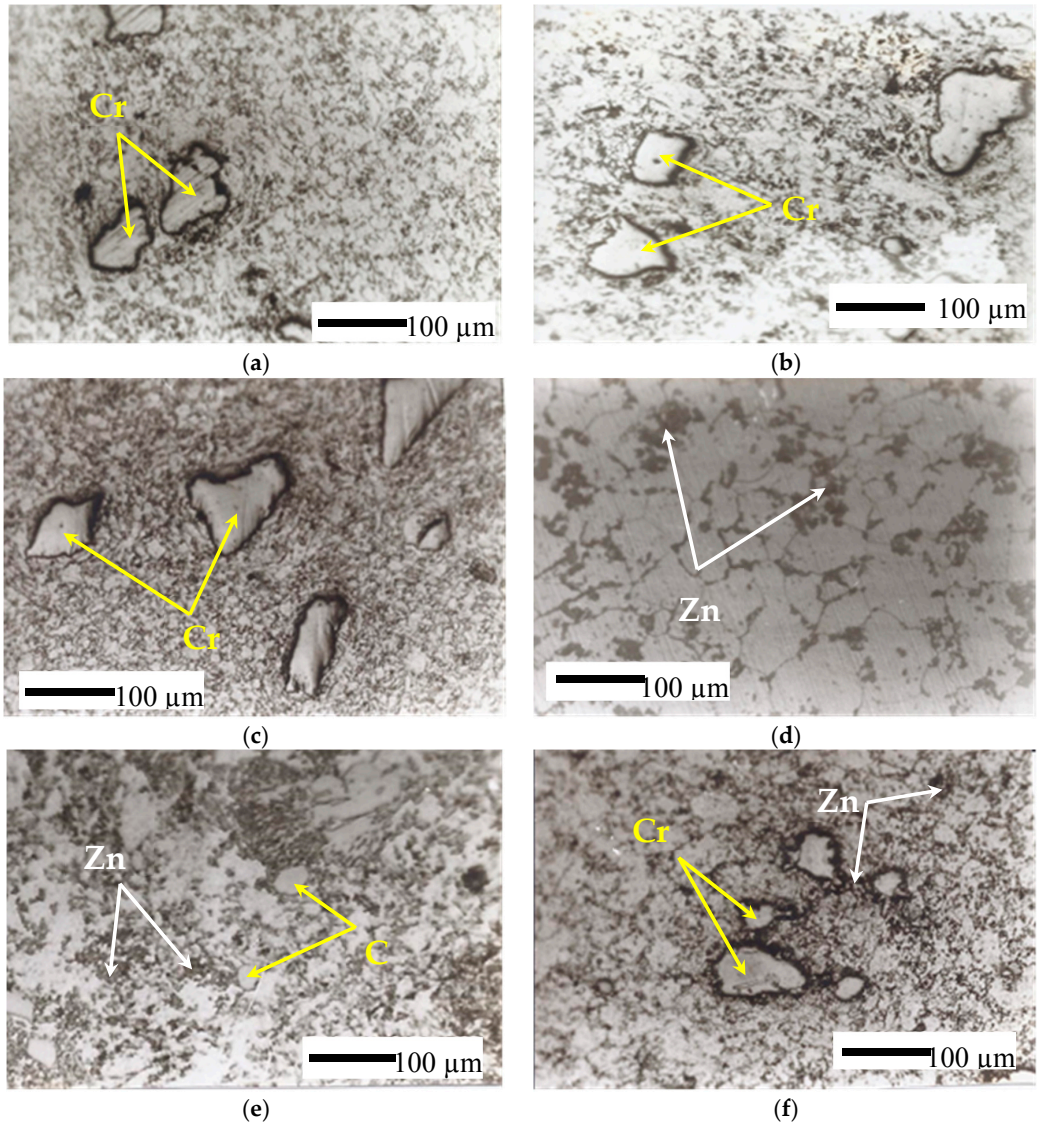

Figure 3. The microstructure of the different heat treated (**a**) Al-5Cr (**b**)Al-7.5Cr (**c**) Al-10Cr (**d**) Al-20Zn (**e**) Al-20Zn-5Cr and (**f**) Al-20Zn-10Cr alloys.

3.2. Microstructural Optical Investigations

There is a difficulty in revealing the grain boundaries in aluminum alloys, especially under heat treatment conditions; therefore, anodizing is required for the lower alloy content grades. Anodizing is an electrolytic etching procedure, which deposits a film on the specimen surface, revealing the grain structure when viewed with crossed polarized light. Using either the Keller's or the Grafet-Sargent reagent for the more highly alloyed grades would lead to a successful etching.

The microstructure of Al-based alloys, which is subjected to heat treatment temperature of 500 °C for 60 min followed by quenching in water at room temperature, is shown in Figure 3. On the other hand, the microstructure of Al-based alloys subjected to extrusion, with an extrusion ratio of 4.6 and solution heat treatment temperature of 500 °C for 60 min followed by quenching in water at room temperature, is shown in Figure 4. The uniform distributions of the Cr and Zn in the homogenous structures were noticed in alloys with Al-based alloys. In addition, it should be reported that surface cracks in the Al-based alloys were very limited. From Figure 3 it is clear that the cold compaction followed by heat treatment technique yielded homogenous microstructure with few pores. In the other hand, the Cr contents in the Al-Zn-Cr ternary system were investigated in Al-20Zn-5Cr and Al-20Zn-10Cr extruded alloys. It is noticed in the micrographs of the extruded billet with heat treatment shown in Figure 4a–f that a fine dispersion of precipitates occurs on the grain surface. In addition, multi-phases were observed in the microstructure in the as-extruded sample, as shown in Figure 4e,f.

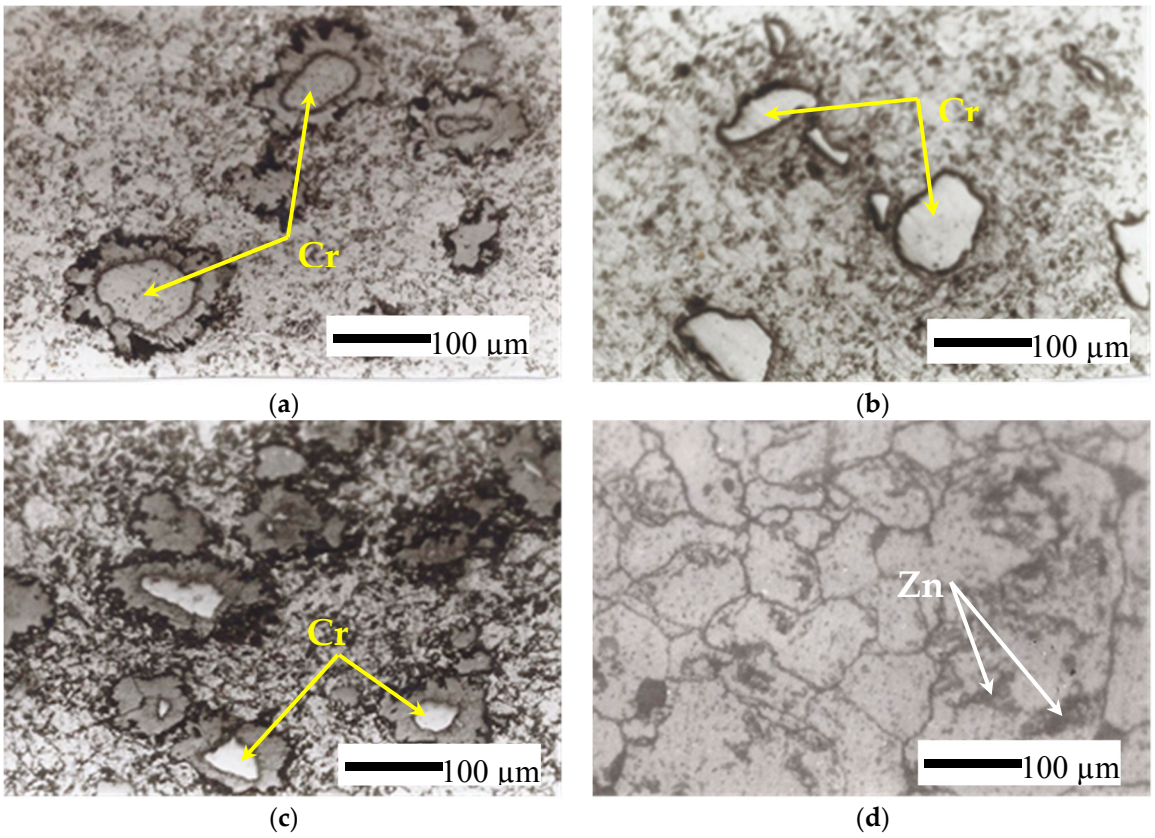

Figure 4. *Cont.*

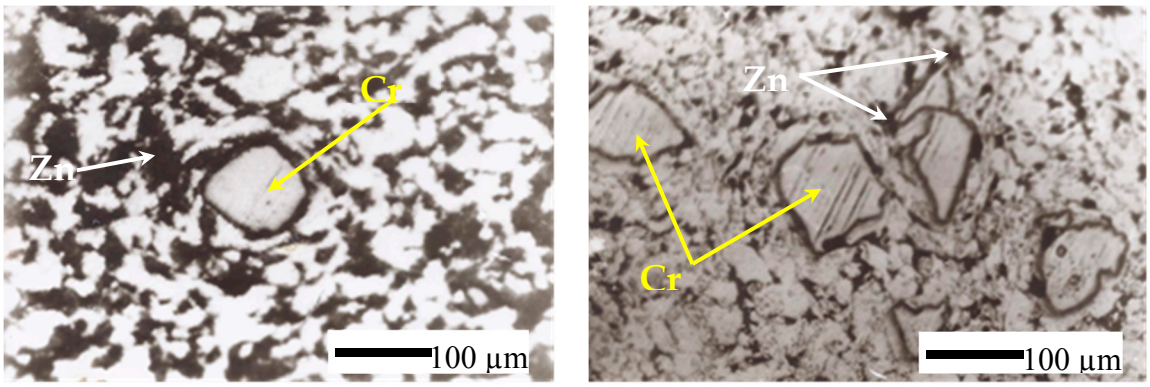

(**e**) (**f**)

Figure 4. The microstructure of the different as-extruded (**a**) Al-5Cr (**b**)Al-7.5Cr (**c**) Al-10Cr (**d**) Al-20Zn (**e**) Al-20Zn-5Cr and (**f**) Al-20Zn-10Cr alloys.

The formation of lots of finely distributed polygonal type of the Cr and Zn particles, in the interface of liquid solid earlier during solidification, may lead to refinement. The process reduces the porosity by the formation of necks between powders, to achieve final elimination of the small pores at the end of the process. It forms new but lower energy solid-solid interfaces with a decrease in the free energy occurring on sintering, where 1 µm particles decreases with 1 cal/g [4]. On a microscopic scale, material transfer was affected by the change in the pressure and the differences in free energy across the curved surface.

It is worth mentioning that the liquid phase was formed at the hot pressing temperature and consolidation was further enhanced, by the isostatic action of the compressive stresses on the compact inside the dies [4,7]. Additionally, diffusion rates were increased by the liquid phase; densification was enhanced by good wetting between liquid and solid components of the alloy system.

3.3. Energy-Dispersive X-ray (EDX) Analysis

The Al-based alloy samples for microscopic examination were prepared using the standard metallographic procedures and were examined at a magnification of 100× by scanning electron microscopy (SEM, Jeol, Peabody, MA, USA). Quantitative energy dispersed X-ray (EDX, Jeol, Peabody, MA, USA) analysis was also performed to analyze the element composition for the different heat treated samples.

After the fabrication process, a Jeol 5400 SEM unit with a link energy dispersive X-ray spectroscopy (EDS) detector (Jeol, Peobody, MA, USA) is attached to observe the particle morphology, size, shape, and agglomeration. The EDX analysis emphasizes this behavior, as shown in Figure 5. The magnified image attached to Figure 5e,f shows that a white large phase was being embedded in a matrix of Al-Zn, as seen from EDX analysis region. The small white phases were mainly Zn particles. After the heat treatment process mentioned above, more homogeneous structure was obtained. The magnified image attached to Figure 5f shows white and dark areas, and the analysis of these areas was given as in EDX analysis region. It can be observed that the white area was Cr rich while the dark was mainly Zn. Figure 3e,f shows micrographs of Al-20Zn-5Cr and Al-20Zn-10Cr alloys, respectively, with heat treatment for one hour followed by water quenching. The liquid Zn during heating indicates homogenous structure, as the Cr particles become smaller than before heating. It shows that the nucleus was enriched with the addition of Cr. The data from EDS spectrum shows that the nature of nucleus was facilitated, as the foreign particle displays a small lattice mismatch in the al-based alloys. The results of calculation for some possible crystallographic orientations on the Cr particles shows that the planar disregistry was low; therefore, Cr can act as the heterogeneous nucleation for Al-based alloys.

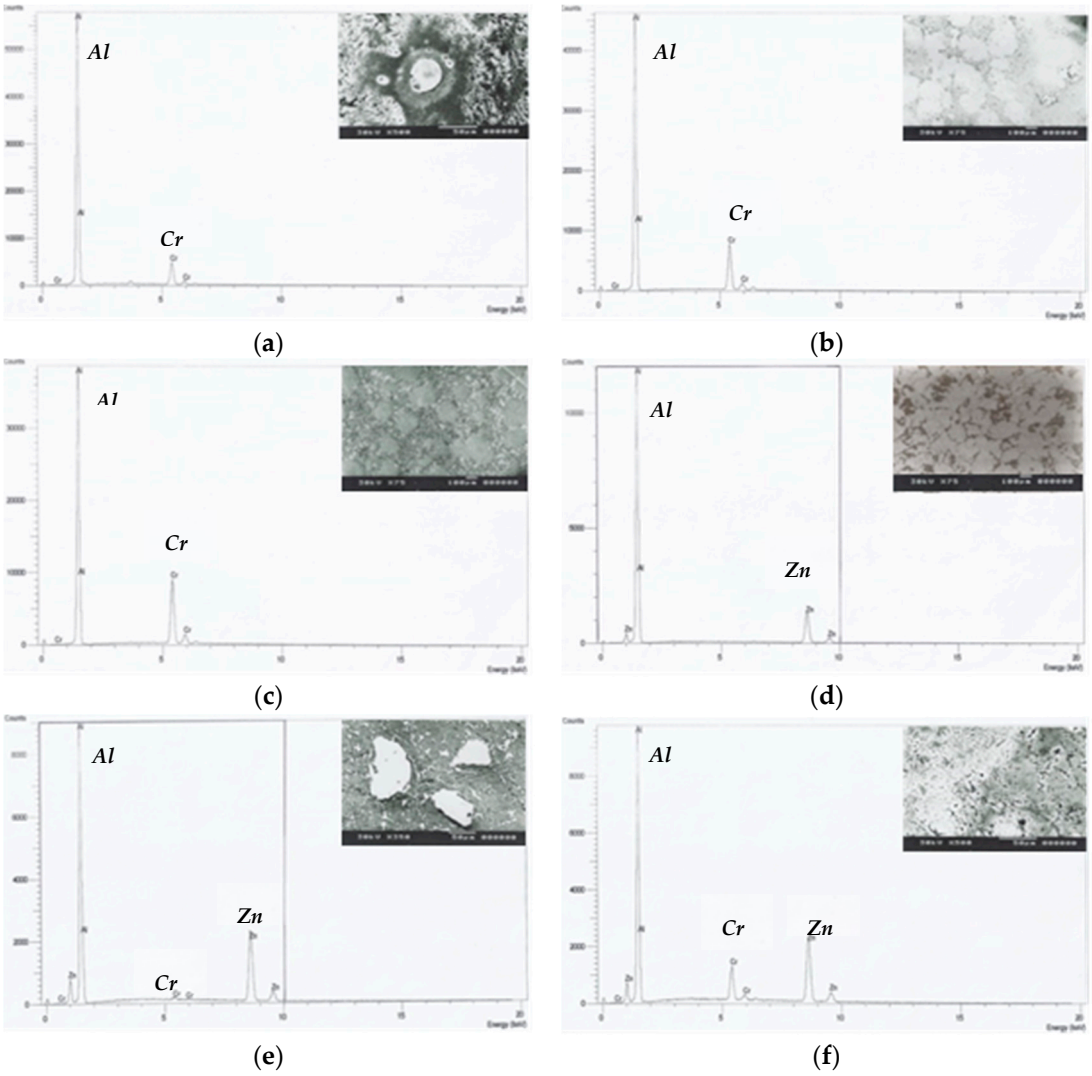

Figure 5. The EDX analysis at the indicated regions with higher magnification for of the different heat treated (**a**) Al-5Cr (**b**) Al-7.5Cr (**c**) Al-10Cr (**d**) Al-20Zn (**e**) Al-20Zn-5Cr and (**f**) Al-20Zn-10Cr alloys.

3.4. Mechanical Properties

Tensile specimens were prepared from the heat treated materials and as extruded states. The gauge length and diameter of the specimens were 30 mm and 6 mm; respectively. Tensile tests were performed at a cross head speed of 2.0 mm/min, which corresponded to an initial strain rate of 1.1×10^{-3} s^{-1}. Tensile tests were conducted at room temperature using materials testing system (MTS) testing machine (model 610), fitted with a 160 kN load cell, operating in the displacement control mode under quasi static loading. The samples were deformed until crashed. For consistency and homogeneity, three identical samples were prepared for each test case and exposed to the same loading conditions. The average test value of all the three samples of the radial crushing strength was reported in Table 1.

Table 1. Average tensile data of Al-base alloys as extrusion and heat treatment with standard deviation SD.

Alloy Composition	As Extruded State				Heat Treated State			
	UTS (σ_u) MPa	SD	Fracture Strain (ε_f) %	SD	UTS (σ_u) MPa	SD	Fracture strain (ε_f) %	SD
Al-5Cr	75	0.1	12	1.2	105	1.4	10	1
Al-7.5Cr	70	0.3	10	1	101	1.4	8	0.78
Al-10Cr	65	0.3	8	0.78	96	0.7	6	0.7
Al-20Zn	188	5.8	18	1.7	185	5.7	16	1.5
Al-20Zn-5Cr	95	0.7	14	1.3	160	4.8	12	1.2
Al-20Zn-10Cr	80	1.4	10	1	143	3.4	8	0.78

Table 1 presents the tensile properties of the materials in both cases of the as-extruded and the heat treated state. For the alloys of Al-Cr without Zn, the ultimate tensile strength and tensile ductility decreases with increasing Cr amount. Comparing the tensile properties of the materials containing Zn with the Zn free counterpart, it is noticed that the addition of Zn resulted in improving both the tensile strength and ductility of Al-20Zn-5Cr and Al-20Zn-10Cr alloys, in the as-extruded state. Thus, the Zn addition appears to be quite favorable, as far as the mechanical properties are concerned. The heat treatment applied to the Zn-containing alloys does not improve their tensile ductility. This was probably related to an improved bonding between the matrix and the Cr as a result of the released local stresses around the Cr particles induced during extrusion.

Rockwell hardness measurements are performed for different produced materials using digital Rockwell hardness tester (SUN-TEC, Novi, MI, USA) at 60 kg load (HRA-60). At least five readings were taken for each case; the averages were recorded to insure consistency and homogeneity throughout the material surface. It was found for all alloys that the the bright phase, which corresponds to δ–phase, had Vickers hardness measurements about two times greater than the corresponding matrix, as presented in Table 2.

Table 2. Rockwell average hardness values Kg/mm^2 for the different Al-base alloys after extrusion and heat treatment with standard deviation SD.

Chemical Composition	Rockwell Hardness As Extruded	SD	Rockwell Hardness Heat Treated at 500 °C	SD
Al-5Cr	8.9	0.9	9.0	0.9
Al-7.5Cr	9.5	1	12.5	1.4
Al-10Cr	9.9	1	14.6	1.4
Al-20Zn	10.4	1	27.6	2.3
Al-20Zn-5Cr	17.4	1.6	30.6	2.5
Al-20Zn-10Cr	16.9	1.5	32.1	2.7

The effect of heating temperatures on hardness for both of the as-extruded and heat treated Al-base alloys were listed in Table 2. The heat treated Al-Zn-Cr alloys demonstrated improvement in hardness values compared with specimen without heat treatment. The heat treatment of Al-20Zn-10Cr alloys at 500 °C had the highest hardness value of 32.1, which represents an increase in hardness for more than 90% compared to that of the specimen without heat treatment. On the other hand, the increase of Cr particles in the Al-base matrix results in an increase of hardness values, as shown in Table 2.

3.5. Corrosion Rate

Corrosion rate were measured for the Al-based alloys using electrochemical polarization. The tests were performed in a corrosion cell, which contained 250 mL of 3.5 wt. % NaCl solutions, at room temperature and scan rate of 0.5 mV/s saturated air. All electrochemical measurements were conducted

using a potentiostat AUTOLAB PGSTATE 30 (Artisan, Champaign, IL, USA) and analyzed using Galvanostat M352 software, at room temperature. Platinum gauze was used, as a counter electrode, and silver/silver chloride was the referenced. The exposed area was 1 cm^2 of all the heat treated and as-extruded Al-based alloys.

An activation-controlled cathodic process occurred in the cathodic branch; the main reaction was hydrogen evolution during the measurements. As the applied potential increased, an activation controlled anodic process was observed. The electrochemical parameters, such as polarization resistance (R_p), were measured. Corrosion current density (I_{corr}) was measured using the linear polarization resistance technique and obtained as a function of R_p, with β_c as the cathodic and β_a anodic Tafel slopes, as $I_{corr} = \beta / R_p$, where β is a constant value and can be calculated by following equation:

$$\beta = \beta_c \times \beta_a / 2.3 \times (\beta_a + \beta_c) \quad (1)$$

The corrosion rate (C_R) expressed in mm per year was obtained from I_{corr} in air saturated sodium chloride solution, according to the Equation (2):

$$C_R = 0.13 \times I_{corr} \times (eq_{wt}) / \rho \quad (2)$$

where eq_{wt} is the equivalent weight, ρ is the density in g/cm^3, and I_{corr} is the corrosion current density determined by the linear polarization method, using the Stern-Geary equation [24]. The corrosion parameters of Al-based alloys are presented in Table 3 for both of the as-extruded and heat treated Al-based alloys.

Table 3. The electrochemical corrosion data for both as extruded and heat treated Al-based alloys.

Chemical Composition	As Extruded		Heat Treated at 500°C	
	C_R mm/year	SD	C_R mm/year	SD
Al pure	0.031	1	–	–
Al-5Cr	0.030	0.9	0.028	0.9
Al-7.5Cr	0.029	0.9	0.027	0.8
Al-10Cr	0.029	0.9	0.026	0.7
Al-20Zn	0.028	0.8	0.024	0.7
Al-20Zn-5Cr	0.026	0.7	0.022	0.6
Al-20Zn-10Cr	0.022	0.6	0.020	0.5

It is noticed that with increase of the Cr and Zn additives in the Al-based alloys, the corrosion rate decreases. As Al-20Zn-10Cr alloys have corrosion rate of 30% less than pure aluminum, the heat treated Al-based alloys had an approximate corrosion rate of 7% less than as-extruded Al-based alloys.

3.6. Wear Resistance

The materials were also subjected to pin-on-disk wear tests under an unlubricated condition, in air and at room temperature. The counter face (the disk) was made of steel with a hardness of RC 32. Before each test, the disk surface was polished by standard metallographic procedure [4,7,25]. The tests were made for different lengths of running times up to 20 min under a constant pressure applied with about 0.127 MPa. Weight loss was calculated using a precise digital analog weight balance (accuracy of ± 0.005 g). Results of the wear resistance for the different Al-based alloys compositions and heat treatment conditions are plotted in Figures 6–8. Figure 6. It shows that increasing Cr content in the binary Al-Cr alloys, for the extruded conditions, improved the wear resistance. Heat treatment of these alloys at 500 °C for one hour decreased the weight loss by about 1.5 times.

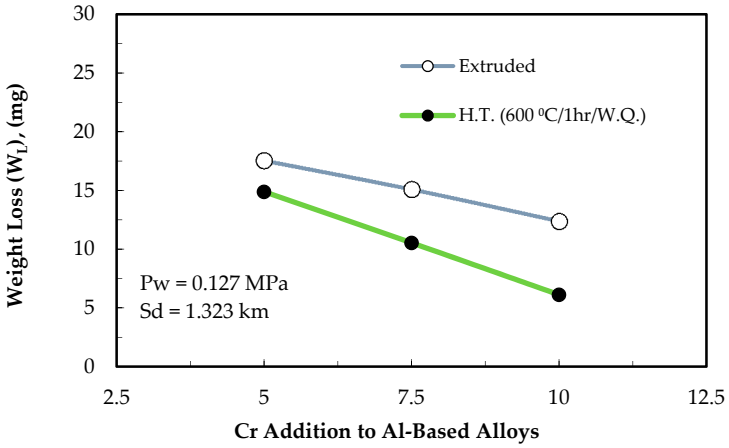

Figure 6. The effect of heat treatment on the weight loss for Al-Cr alloys.

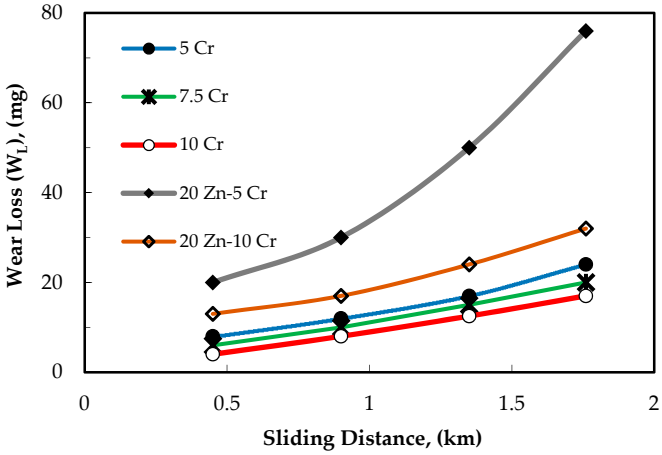

Figure 7. The weight loss versus sliding distance of Al-base alloys in the as-extruded condition.

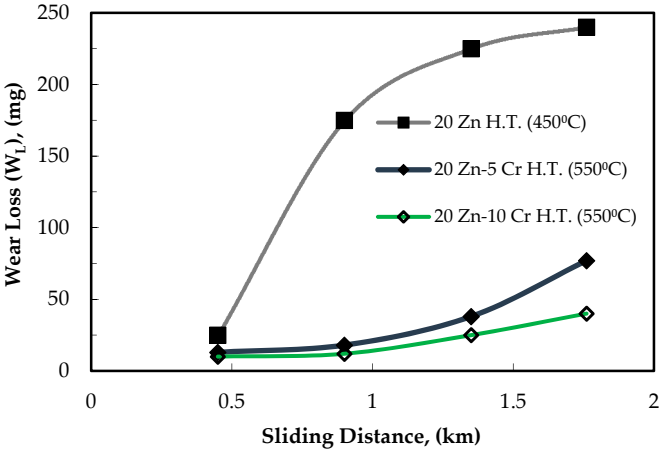

Figure 8. The effect of Cr addition on the weight loss of heat treated Al-20Zn alloys.

The microstructure shown in Figure 3a indicates that heat treatment of the binary Al-Cr alloys led to a diffusion of aluminum in the Cr particles, resulting in gradual alloying of the Cr particle. It is possible that some Cr particles were dissolved in Al-based alloys, which resulted in alloy hardening and; consequently, an increase in the wear resistance. In the ternary alloys of Al-Zn-Cr, the addition of Zn increases the weight loss for the alloys containing 5 or 10 wt. % Cr, as shown in Figure 7. This

effect was clearer for the alloys containing 5 wt. % Cr. The weight loss of these alloys was about 2 times higher compared to the 10 wt. % Cr ternary alloys. In the as-extruded condition, the addition of Zn to the Al-Cr alloys resulted in a higher degree of homogeneity in the microstructure, as shown in Figure 3e,f; however, Cr is a hard metal and is expected to improve wear resistance.

The wear resistance results for the heat treated Al-20Zn alloys and Al-20Zn alloys, containing 5 and 10 wt. % Cr, was plotted in Figure 8. The wear resistance of the Al-20Zn-Cr alloys were found to be around 5 to 8 fold greater than the Al-20Zn alloys, after 1.76 km sliding distance. The presence of 20 wt. % Zn in the Al-Cr alloys during heat treatment enhanced the inter-diffusion process and formation of homogenous Al-Zn-Cr alloys, as shown in Figure 3e. The Cr particles have almost disappeared although EDX analysis, in Figure 8c,d, showed two phase alloys with different Cr contents. As mentioned above, the addition of Cr to the base alloy increased the hardness compared to the Al-20Zn alloys.

4. Conclusions

Based on the results of the present study, the following conclusions could be reached:

1. Binary Al-Cr alloys from powders, heat-treated at different conditions, could not establish a homogenous microstructure.
2. The presence of 20 wt. % Zn in the Al-Cr alloys enhanced the interdiffusion and densification process during heat treatment, due to the formation of a liquid phase leading to a homogenius microstructure.
3. Both Zn addition and the heat treatment temperature affect the hardness values and the structure of the Al-base matrix
4. Under tension load, improvement in the strength of Al-Cr alloys was obtained after Zn addition and the heat-treatment process.
5. The increase of the Cr and Zn additives in the Al-based alloys would result in a decrease in the corrosion rate. As Al-20Zn-10Cr alloys have corrosion rate of 30% less than pure aluminum, the heat treated Al-based alloys had an approximate corrosion rate of 7% less than as-extruded Al-based alloys.
6. The wear resistance of the ternary Al-Zn-Cr heat treated at 500 °C for one hour was about 5 times higher than that of the binary Al-Zn alloys. The alloy of Al-20Zn-5Cr, heat-treated at 500 °C for one hour followed by water quenching, exhibited the highest wear resistance among the investigated alloys.

Author Contributions: All authors contributed equally in designing and manufacturing of the studied alloys, conceiving, designing and performing the experiments, collecting and analyzing the data, and finally discussion association of the results. I would like to also indicate that the corresponding author was responsible for addressing all reviewers' remarks and journal correspondence.

Conflicts of Interest: The authors also declare no conflict of interest.

References

1. Liu, S.; Zhong, Q.; Zhang, Y.; Liu, W.; Zhang, X.; Deng, D. Investigation of quench sensitivity of high strength Al-Zn-Mg-Cu alloys by time–temperature-properties diagrams. *Mater. Des.* **2010**, *31*, 3116–3120. [CrossRef]
2. Ezuber, H.; El-Houd, A.; El-Shawesh, F. A study on the corrosion behavior of aluminum alloys in seawater. *Mater. Des.* **2008**, *29*, 801–805. [CrossRef]
3. Kalkanl, A.; Yılmaz, S. Synthesis and characterization of aluminum alloy 7075 reinforced with silicon carbide particulates. *Mater. Des.* **2008**, *29*, 775–780. [CrossRef]
4. Nassef, A.; El-Hadek, M. Mechanics of hot pressed aluminum composites. *Int. J. Adv. Manuf. Technol.* **2015**, *76*, 1905–1912. [CrossRef]
5. El-Hadek, M.; Kassem, M. Failure behavior of Cu-Ti-Zr-based bulk metallic glass alloys. *J. Mater. Sci.* **2009**, *44*, 1127–1136. [CrossRef]

6. El-Hadek, M.; Kaytbay, S. Al_2O_3 Particle Size Effect on Reinforced Copper Alloys: An Experimental Study. *Strain* **2009**, *45*, 506–515. [CrossRef]
7. Nassef, A.; El-Hadek, M. Microstructure and Mechanical Behavior of Hot Pressed Cu-Sn Powder Alloys. *Adv. Mater. Sci. Eng.* **2016**, *2016*, 1–10. [CrossRef]
8. Kurtuldu, G.; Jarry, P.; Rappaz, M. Influence of Cr on the nucleation of primary Al and formation of twinned dendrites in Al-Zn-Cr alloys: Can icosahedral solid clusters play a role? *Acta Mater.* **2013**, *61*, 7098–7108. [CrossRef]
9. Kurtuldu, G.; Jarry, P.; Rappaz, M. Influence of icosahedral short range order on diffusion in liquids: A study on Al-Zn-Cr alloys. *Acta Mater.* **2016**, *115*, 423–433. [CrossRef]
10. Del Arco, M.; Rives, V.; Trujillano, R.; Malet, P. Thermal behavior of Zn-Cr layered double hydroxides with hydrotalcite-like structures containing carbonate or decavanadate. *J. Mater. Chem.* **1996**, *6*, 1419–1428. [CrossRef]
11. Peng, G.; Chen, K.; Fang, H.; Chen, S. Effect of Cr and Yb additions on microstructure and properties of low copper Al-Zn-Mg-Cu-Zr alloy. *Mater. Des.* **2012**, *36*, 279–283. [CrossRef]
12. He, Z.; Su, X.; Peng, H.; Liu, L.; Wu, C.; Wang, J. 600 °C isothermal section of the Al-Cr-Zn ternary phase diagram. *J. Alloys Compd.* **2015**, *649*, 1239–1245. [CrossRef]
13. Li, C.B.; Han, S.Q.; Liu, S.D.; Deng, Y.L.; Zhang, X.M. Grain structure effect on quench sensitivity of Al-Zn-Mg-Cu-Cr alloy. *Trans. Nonferr. Met. Soc. China* **2016**, *26*, 2276–2282. [CrossRef]
14. Fourmentin, R.; Avettand-Fènoël, M.N.; Reumont, G.; Perrot, P. The Fe-Zn-Al-Cr system and its impact on the galvanizing process in chromium-added zinc baths. *J. Mater. Sci.* **2008**, *43*, 6872–6880. [CrossRef]
15. Shaha, S.K.; Czerwinski, F.; Kasprzak, W.; Friedman, J.; Chen, D.L. Ageing characteristics and high-temperature tensile properties of Al-Si-Cu-Mg alloys with micro-additions of Cr, Ti, V and Zr. *Mater. Sci. Eng. A* **2016**, *652*, 353–364. [CrossRef]
16. Shin, S.-S.; Lim, K.-M.; Park, I.-M. Effects of high Zn content on the microstructure and mechanical properties of Al-Zn-Cu gravity-cast alloys. *Mater. Sci. Eng. A* **2017**, *679*, 340–349. [CrossRef]
17. Chinh, N.Q.; Jenei, P.; Gubicza, J.; Bobrukb, E.V.; Valiev, R.Z.; Langdon, T.G. Influence of Zn content on the microstructure and mechanical performance of ultrafine-grained Al-Zn alloys processed by high-pressure torsion. *Mater. Lett.* **2017**, *186*, 334–337. [CrossRef]
18. Staišiūnas, L.; Miečinskas, P.; Leinartas, K.; Selskis, A.; Griguceviči enė, A.; Juzeliūnas, E. Sputter-deposited Mg-Al-Zn-Cr alloys—Electrochemical characterization of single films and multilayer protection of AZ31 magnesium alloy. *J. Corros. Sci.* **2014**, *80*, 487–493. [CrossRef]
19. Wang, H.; Zhang, R.; Hu, X.; Wang, C.A.; Huang, Y. Characterization of a powder metallurgy SiC/Cu-Al composite. *J. Mater. Process. Technol.* **2008**, *197*, 43–48. [CrossRef]
20. Ogel, B.; Gurbuz, R. Microstructural characterization and tensile properties of hot pressed Al-SiC composites prepared from pure Al and Cu powders. *Mater. Sci. Eng. A* **2001**, *301*, 213–220. [CrossRef]
21. Chang, Y.; Sun, W.; Xiong, X.; Chen, Z.; Wang, Y.; Hao, Z.; Xu, Y. A novel design of Al-Cr alloy surface sealing for ablation resistant C/C-ZrC-SiC composite. *J. Eur. Ceram. Soc.* **2017**, *37*, 859–864. [CrossRef]
22. El-Hadek, M.; Kassem, M. Characterization of strengthened rapidly quenched Zr-based alloys. *Int. J. Mech. Mater. Des.* **2008**, *4*, 279–289. [CrossRef]
23. El-Hadek, M.; Kaytbay, S. Fracture properties of SPS tungsten copper powder composites. *Metall. Mater. Trans. A* **2013**, *44*, 544–551. [CrossRef]
24. Ozyılmaz, A.T.; Kardas, G.; Erbil, M.; Yazici, B. The corrosion performance of polyaniline on nickel plated mild steel. *Appl. Surf. Sci.* **2005**, *242*, 97–106. [CrossRef]
25. Kaytbay, S.; El-Hadek, M. Wear resistance and fracture mechanics of WC–Co composites. *Int. J. Mater. Res.* **2014**, *105*, 557–565. [CrossRef]